DEGREE PROJECT, IN MECHATRONICS , SECOND LEVEL
STOCKHOLM, *SWEDEN 2015*

Development and evaluation of a six degrees of freedom model of a 155 mm artillery projectile

MARCUS THURESSON

KTH ROYAL INSTITUTE OF TECHNOLOGY

INDUSTRIAL ENGINEERING AND MANAGEMENT

Master of Science Thesis MMK 2015:94 MDA 523

KTH Industrial Engineering and Management

Development and evaluation of a six degrees of freedom model of a 155 mm artillery projectile

Marcus Thuresson

Approved	Examiner	Supervisor
2015-sept-16	Lei Feng	Mohammad K. Khansari
	Commissioner	Contact person
	Swedish Defense University	Björn Persson

Abstract

In this Master Thesis, the author has evaluated a six degrees of freedom model of a 155 mm artillery projectile commonly used in the Swedish Armed Forces and compared it to a modified point mass trajectory model of the same projectile. Uncertainties in the six degrees of freedom model were assumed to evaluate the precision of the model compared to the precision of the real fire data. The models were simulated using the software FLAMES, that uses a spherical earth model, terrain data and measured atmospheric conditions. The real fire data comes from a number of fire series performed by the Swedish Armed Forces in 2001.

The results showed that six degrees of freedom model was accurate in length but had an upwards 35 % error in drift when verified against a firetable. When the six degrees of freedom model was compared to a modified point mass model and real fire hits the mean distance to target was about 250 m. A plausible reason for this large mean distance is that the in data used in this thesis had to low order of accuracy. This thesis also showed a large difference in angle of attack between the models during high elevation simulations as well as when there was wind present. The results for the six degrees of freedom model with uncertainties showed that 90 % of all projectiles hit within a 50 m x 75 m ellipse, at a simulated fire distance of about 16 km.

Examensarbete MMK 2015:94 MDA 523

KTH Industriell teknik och management

Utveckling och evaluering av en sex frihetsgrads modell av en 155 mm artilleri granat

Marcus Thuresson

Godkänt	Examinator	Handledare
2015-sept-16	Lei Feng	Mohammad K. Khansari
	Uppdragsgivare	Kontaktperson
	Försvarshögskolan	Björn Persson

Sammanfattning

I detta examensarbete har författaren utvärderat en sex frihetsgrads modell av en 155 mm artillerigranat som används av den svenska Försvarsmakten och jämfört den med en modifierad punktmassa modell av samma projektil. Osäkerheter antogs i sex frihetsgrads-modellen för att utvärdera modellens precision mot verklig precision. Modellerna simulerades i programmet FLAMES, med en sfärisk jordmodell, terräng data och uppmätta atmosfäriska förhållanden. Skjutdatan som användes som jämförelse kommer från en skjutning i Boden år 2001 utfört av den svenska Försvarsmakten.

Resultaten visade att sex frihetsgrads-modellen var korrekt i längd, men hade uppåt 35 % fel i drift när den verifierades mot en skjuttabell. När sex frihetsgrads-modellen jämfördes med skjutdata från en riktig skjutning var medelavståndet från riktigt nedslag till nedslag för sex frihetsgradsmodellen ca 250m. En trolig orsak till det stora medelavståndet är att indata som användes hade en noggrannhet som inte var tillräckligt hög. Detta examensarbete visade också en stor skillnad i anfallsvinkeln mellan modellerna under höga skjutvinklar samt när det fanns vind närvarande. Resultaten för sex frihetsgrads-modellen med osäkerheter visade att 90 % av alla projektiler träffar inom en 50 m x 75 m ellips, vid skjutning på cirka 16 km avstånd.

FOREWORD

This thesis was performed in the spring of 2015 at the Swedish Defense University located in Stockholm. The Swedish Defense University educates future and current military officers mainly from the Swedish Armed Forces, but the university is no longer a part of the Swedish Armed Forces. I (the author, Marcus Thuresson) was conscripted into the Swedish Armed Forces in 2009-2010, where I served in a howitzer platoon. Therefore I have firsthand knowledge of how a howitzer functions and which other parameters are needed for a fire mission, knowledge that has been very valuable during this project.

I would like to thank my supervisors, Björn Persson at the Swedish Defense University and Mohammad Khodobakhshian Khansari at The Royal Institute of Technology. I have also received additional support from employees at BAE systems located in Karlskoga, by Thomas Pettersson and Marcus Eliasson.

NOMENCLATURE

Here are the Notations and Abbreviations that are used in this Master thesis.

Notations

Symbol *Description*

V	Velocity (m/s)
W	Wind speed (m/s)
υ	Total velocity (m/s)
ρ	Density (kg/m^3)
S	Projected front area of the projectile (m^2)
m	Mass (kg)
v	Velocity relative to wind (m/s)
d	Diameter of the projectile (m)
h	Angular momentum ($Kg\ m^2/s$)
x	Unit vector along the projectile's axis of symmetry
g	Acceleration due to gravity (m/s^2)
I_z	Transverse moment of Inertia ($Kg\ m^2$)
I_x	Axial moment of Inertia ($Kg\ m^2$)
p	Axial rotation speed (rad/s)
C_D	Drag force coefficient
C_{L_α}	Lift force coefficient
$C_{N_{p\alpha}}$	Magnus force coefficient
$C_{N_{\dot{\alpha}}}$	Normal force coefficient derivate
C_{lp}	Spin damping moment coefficient

C_{M_α}	Overturning moment coefficient
$C_{M_{p\alpha}}$	Magnus moment coefficient
C_{M_q}	Pitch damping moment coefficient
$C_{M_{\dot{\alpha}}}$	Overturning moment coefficient derivative

Terminology

Term	*Description*
Howitzer	Artillery cannon of medium muzzle velocity, capable of firing with low and high trajectories.
Archer	A self-propelled howitzer currently used by the Swedish Armed Forces.
FH77B	A retired towed Swedish howitzer.
m/sgr77	Explosive shell used by the Swedish Armed Forces.
Yaw of repose, angle of equilibrium	Angle between projectile axis and the direction of travel, in this thesis the yaw of repose is a vector. Yaw of repose is a concept used mainly when using the modified point mass model.
Angle of attack	Angle between the projectile's axis and the direction of travel. The angle of attack is not a vector but expressed in radians or degrees.
alpha, beta	Pitch and yaw components of the angle of attack. Expressed in radians or degrees.
6-DOF	Six Degrees Of Freedom.
MPMM	Modified Point Mass Model.
FLAMES	Flexible Analysis, Modeling and Exercise System, modelling software mainly used for military purposes.

Fire data	Consists of coefficients, atmospheric data and projectile properties. Also included was a real fire scenario, including coordinates of the howitzers, targets and actual hits.
Fire table	A table that lists length, drift, time of flight etcetera for different gun powder charges. A fire table can be used to fire if no trajectory software is available.

TABLE OF CONTENTS

1 INTRODUCTION

1.1 Background

A crucial part of any army, today and historically, has been its artillery. In the ancient world, the roman legions fielded mechanical equipment such as the ballista that could hurl boulders or large arrows hundreds of meters into the enemy ranks [1]. The discovery of gunpowder in China in the 9th century [2] led to the development of artillery that used gunpowder as propulsion to launch projectiles. Today, the general role for artillery on the battlefield is to provide fire support, defined by NATO as "the application of fire, coordinated with the maneuver of forces to destroy, neutralize or suppress the enemy" [3].

Artillery is a term for any long range cannons that can fire unguided and guided projectiles for many kilometers, with mixed accuracy. In a modern army precision is sought-after, as it is both more cost effective (fewer artillery pieces and projectiles needed) and also minimizes the risk of hitting friendly or non-combatant units [4]. In order to hit a target at long range with good accuracy, the trajectory of the projectile must be calculated. This was done by using different models that takes into account the current conditions at the firing site, such as weather, projectile mass, earth's rotation and aerodynamic properties of the projectile. Modern artillery shells are spin-stabilized, which puts higher demands on the number of freedoms needed to accurately model the trajectory. Different models approach this problem in different ways, and this work will focus on the Six Degrees Of Freedom model (6-DOF) and the Modified Point Mass Model (MPMM). The MPMM is a simplification of the 6-DOF model, and has fast computing speeds; the 6-DOF model is more complex and should be more precise. The MPMM for an m/sgr77 projectile already exists at the Swedish Defense University, abbreviated FHS in Swedish, since it was made as a part of a thesis project in 2014 [5]. However, no 6-DOF model of an m/sgr77 artillery projectile existed at the beginning of this thesis project at the Swedish Defense University.

1.2 Purpose

The purpose of this master thesis was to implement a 6-DOF (three rotational DOF and three linear DOF) model of an SGR 77 spin-stabilized projectile in free flight, with as few assumptions as possible. The 6-DOF model can also be used in further research at the Swedish Defense University concerning guided projectiles, as a 6-DOF model is needed when dynamic wings are added. The Swedish Defense University was also interested in implementing a 6-DOF model to certain artillery courses at the Swedish Defense University attended by military officers. The idea was that a 6-DOF model that depicts all forces and moments during the trajectory can increase the physical understanding of which parameters has the biggest impact on the flight trajectory. The 6-DOF model was also to be compared to an existing MPMM, to determine if the less complex and fast model (the MPMM) had acceptable accuracy compared to the 6-DOF model. The howitzers precision due to uncertainties was investigated, to determine probability of hit area around the target location.

1.3 Problem description

An MPMM exists today at the Swedish Defense University, which is a four degrees of freedom model. The MPMM (continuously shortened to as MPMM later in the text) is a fast and simple model that requires few inputs, but it assumes that the projectile is stable during flight and does not model the projectile's rotational behavior. The 6-DOF model requires more aerodynamic coefficients and significantly more computing power, but it is also said to be the most accurate trajectory model [6]. Therefore this thesis will compare the MPMM with the 6-DOF model, to see if the MPMM can be used instead in certain scenarios, i.e. when the projectiles rotational behavior is not being examined and when short computing times are needed.

The 6-DOF model will be verified compared to a fire table for an FH77B; comparing distance traveled and drift for a number of different initial velocities and elevation angles.

A model requires good input to generate reliable and realistic results; therefore a number of uncertainties were added to the model. The uncertainties are in the howitzers position, azimuth and elevation angles, projectile mass, v0 radar system (measures initial velocity of the projectiles as it leaves the barrel) and metrology. These uncertainties were used to estimate the howitzers precision.

1.4 Method

The 6-DOF model was written in C++, and the simulation software used was FLAMES (Flexible Analysis, Modeling and Exercise System) [7]. The physical equations needed for the 6-DOF model were based on those written by Robert L. McCoy in "Modern Exterior Ballistics" [6].

The list below summarizes the working process;

1. A literature study of the field was made to retrieve information on which forces, moments and inputs that were needed to get an accurate 6-DOF model.
2. Coefficient data for an m/sgr77 projectile was gathered in table format. The data was then interpolated by using splines between the data points; this was done to have interpolated data between the actual data points.
3. Time step and suitable integration method. The time step was determined by running multiple tests with different simulation time and by examining the results. If the results were very similar, the highest time step that generated a precise result was chosen.
4. 6-DOF simulation software were written in C++ and implemented in FLAMES, and verified the model. This was be done by both comparing it to real fire data and by comparing the 6-DOF model to a fire table from an FH77B.

5. Uncertainties that exist in the real world but not in the mathematical equations were identified and assumed, and added those to the current 6-DOF model.
6. Ran 6-DOF simulation multiple times, using all previously assumed uncertainties, to determine the precision, by using a Monte Carlo method.
7. Logged results, and plotted them using MATLAB.
8. Present results, discussion, conclusions and future improvements.

1.5 Limitations

- Small real fire data sample size. All data comes from the same day and about the same firing distance.
- Uncertainties in howitzer performance, as they are assumed and not based on real models of their behavior.
- No recorded pressure exists in the fire data; therefore the pressure is being calculated internally in FLAMES by using recorded temperature as input.
- The 6-DOF model was using the US standard atmosphere from 1976, however the fire table used to verify the model used the Swedish Armed Forces standardized atmosphere from 1948.

1.6 Previous work

The foundations of the 6-DOF model were presented in 1920, by Fowler, Gallop and Richmond. However, the 6-DOF equations could not be used practically until the appearance of the modern high speed computer, practical 6-DOF programs did not appear until the late 1950s and early 1960s [6]. The 6-DOF equations used in this work was presented in the 1950s by R.H. Kent at the Ballistic Research Laboratory [8] and updated by Robert L. McCoy [6]. The field of exterior ballistics has been researched heavily by the defense industry and various national armed forces, but far from everything gets published. The MPMM and the 6-DOF model are two common high accuracy models and they have been studied extensively, but the impact of dynamic atmospheric data and comparisons with real fire data are scarce in the academic world.

The code for the MPMM was mostly written by Otto Nordgren in 2014 as a part of a thesis project performed at FHS [5]. Nordgren used the same coefficient data and fire data that were used throughout this thesis. Nordgren concluded that the MPMM corresponds well to real fire data.

2 MODELLING CONCEPT

In order to predict the trajectory of a projectile, a model is needed that describes the motion of the projectile during its flight. This thesis focused on two different models; the 6-DOF model and the MPMM. The MPMM does not describe all degrees of freedom during the flight path, but focuses on the part of the motion that has biggest effect on the trajectory. The MPMM model is less complex and is therefore faster to solve than the 6-DOF model. Figure 1 shows how the unit vectors ***x, y, z*** are defined.

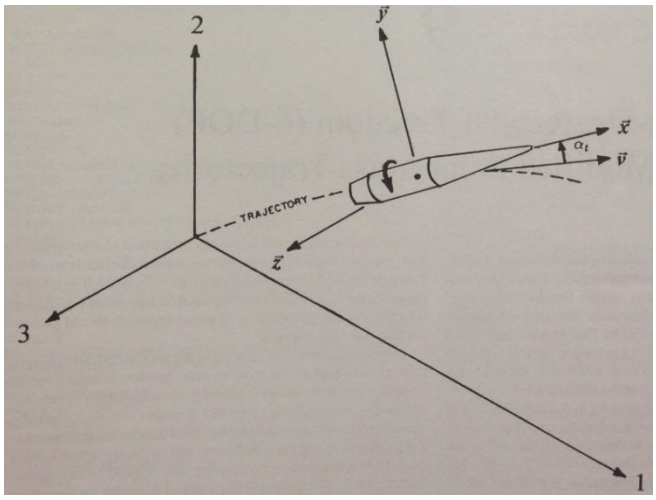

Figure 1. This Figure shows how the body coordinate axes x, y, z are defined. McCoy uses a coordinate system that is fixated in the howitzers firing position. The picture is a photocopy from "*Modern Exterior Ballistics*" by McCoy.

2.1 External ballistics introduction

External ballistics covers the flightpath from the moment the projectile leaves the barrel until impact. By applying external ballistics equations of motion it is possible to predict where the point of impact will be. Due to different projectile shapes there are two main strategies on how to make a projectile stable during its flight. Some projectiles have the center of mass located in front of the center of pressure; such as arrows and mortar grenades, which has a positive effect on projectile stability. In that case it is enough to place fins on the rear of the projectile to make sure that the center of pressure is located behind the center of mass [6], and thus generating a stable projectile. The airflow will in that case act as a stabilizing force.

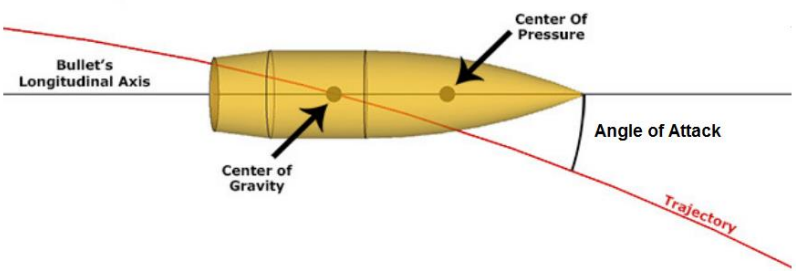

Figure 2. This figure illustrates the approximate locations of centers of pressure and mass. The angle of attack can also be seen, which is the angle between the projectile's axis of symmetry and the trajectory direction. [16]

However, artillery projectiles and standard rifle and pistol ammunition have the center of mass located behind the center of pressure, see Figure 2, which has negative impact on projectile stability. Rifle and artillery projectiles usually travel faster than Mach 1 (faster than the speed of sound), and the drag can be significantly reduced by having a long projectile with a long nose at those speeds [6].

As a side effect, the center of mass is therefore located behind the center of pressure. Since the center of pressure is located in the front, some forces will create destabilizing moments around the center of mass, which will make the projectile tumble during flight. The solution to this problem is spin-stabilizing, i.e. the projectile will spin around its axis of symmetry at high rotational speed. This rotation will introduce gyroscopic stability to the projectile, which will cause the projectile's nose to undergo precession around the direction of travel with decreasing amplitude. The same effect can be seen with a spinning top, it will fall to its side if it is not spinning, but remain upwards as long as it is spinning fast enough. Another effect of the gyroscopic stability is called yaw of equilibrium, because the projectile's nose will point to the right of the direction of travel for projectiles with a right hand direction of rotation. This effect will cause projectiles with a right hand twist to drift to the right [6], see Figure 3.

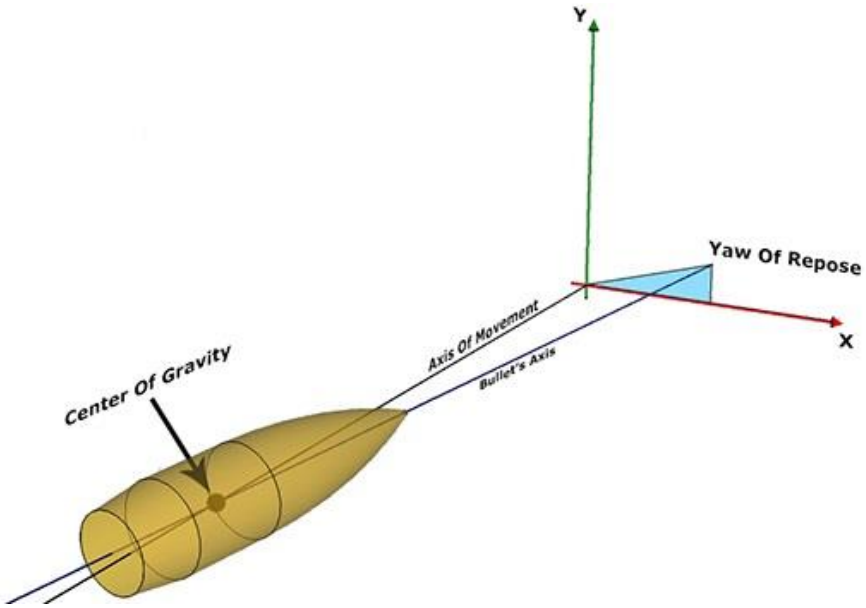

Figure 3. Illustration of the typical direction of the yaw of repose vector. [17]

2.2 6-DOF trajectory model

In the 6-DOF model each degree can be adequately described in every position of its flightpath. This model is the most complex model in the field of exterior ballistics, and gives the most accurate solution possible, provided that all the aerodynamic forces, moments and initial conditions are known to a high degree of accuracy [6]. The projectile is assumed to be rigid (non-flexible) and rotationally symmetric. A rotationally symmetric body gives that the transverse moment of inertia I_y and I_z are equal. Bold characters denote vectors.

The 6-DOF model contains two vector differential equations of motion, influenced by significant aerodynamic forces, wind, gravity, Coriolis Effect, and moments.
There are two highly coupled differential equations, the first (1) for the linear DOF and latter (2) for the rotational DOF [6].

$$\frac{d\boldsymbol{V}}{dt} = -\frac{\rho v S C_D}{2m}\boldsymbol{v} + \frac{\rho S C_{L_\alpha}}{2m}[v^2\boldsymbol{x} - (\boldsymbol{v}\cdot\boldsymbol{x})\boldsymbol{v}] - \frac{\rho S d C_{N_{p\alpha}}}{2m}\frac{I_y}{I_x}(\boldsymbol{h}\cdot\boldsymbol{x})(\boldsymbol{x}\times\boldsymbol{v}) + \boldsymbol{g} + \boldsymbol{\Lambda} \tag{1}$$

Equation (1) is the linear differential equation, that takes into account drag force, lift force, Magnus force, gravity force and the Coriolis Effect. All forces have been divided with mass to get accelerations.

$$\frac{d\boldsymbol{h}}{dt} = \frac{\rho v S d^2 C_{lp}}{2I_x}(\boldsymbol{h}\cdot\boldsymbol{x})\boldsymbol{x} + \frac{\rho v S d C_{M_\alpha}}{2I_y}(\boldsymbol{V}\times\boldsymbol{x}) + \frac{\rho S d^2 C_{M_{p\alpha}}}{2I_x}(\boldsymbol{h}\cdot\boldsymbol{x})[\boldsymbol{v} - (\boldsymbol{v}\cdot\boldsymbol{x})\boldsymbol{x}] + \frac{\rho v S d^2 (C_{M_q} + C_{M_{\dot\alpha}})}{2I_y}[\boldsymbol{h} - (\boldsymbol{h}\cdot\boldsymbol{x})\boldsymbol{x}] \tag{2}$$

Equation (2) is the rotational differential equation, including spin damping moment, overturning moment, Magnus moment and pitch damping moment. All moments has been divided with their corresponding moment of inertia to get rotational accelerations.

$\boldsymbol{v}$ is defined as

$$\boldsymbol{v} = \boldsymbol{V} - \boldsymbol{W} \tag{3}$$

and

$$v = \sqrt{v_x + v_y + v_z} \tag{4}$$

Where v_x, v_y, v_z are vector components of $\boldsymbol{v}$ from (3).

To start the calculations certain initial conditions needs to be set. The angular momentum is given by

$$\boldsymbol{h} = \frac{I_x}{I_y}p\cdot\boldsymbol{x} + (\boldsymbol{x}\times\frac{d\boldsymbol{x}}{dt}) \tag{5}$$

If no lateral throw off is assumed to exist, the initial angular momentum can be simplified to

$$h_{x0} = \frac{I_x}{I_y} p \tag{6}$$

This would give the initial angular momentum vector

$$\boldsymbol{h_0} = [\frac{I_x}{I_y} p, 0, 0] \tag{7}$$

The initial condition for the velocity vector is

$$\boldsymbol{V_0} = [V_{x0}, V_{y0}\ , V_{z0}] \tag{8}$$

The direction change of the $\boldsymbol{x}$ vector is defined as

$$\frac{d\boldsymbol{x}}{dt} = \boldsymbol{h} \times \boldsymbol{x} \tag{9}$$

Equation 10 gives the new direction of the projectile's unit vector.

$$\boldsymbol{x}_{new} = \boldsymbol{x} + \frac{d\boldsymbol{x}}{dt} \cdot dt \tag{10}$$

The angle of attack for the 6-DOF model is defined as

$$\alpha_t = \sqrt{\alpha^2 + \beta^2} \tag{11}$$

Where α and β are pitch and yaw components respectively of the angle of attack angle, see Figure 2.

2.3 Modified point mass trajectory model

The MPMM is a four degrees of freedom model that is less complex and therefore computational faster. The MPMM was developed during the 1960s simply because of the

long computer run times for the 6-DOF model [6]. It is a simplification of the 6-DOF model [9]. It calculates all three linear degrees of freedom similarly to the 6-DOF model, but only approximates the yaw of equilibrium, commonly called yaw of repose [9]. The MPMM requires less aerodynamic coefficients as fewer forces and moments are used in the equations.

The differential equation for the linear movement stated as

$$\frac{d\boldsymbol{V}}{dt} = -\frac{\rho v S C_D}{2m}\boldsymbol{v} + \frac{\rho S C_{L_\alpha}}{2m} v^2 \boldsymbol{\alpha_R} + \frac{\rho S d C_{N_{p\alpha}} p}{2m} v(\boldsymbol{x} \times \boldsymbol{\alpha_R}) + \boldsymbol{g} + \boldsymbol{\Lambda} \tag{12}$$

The differential equation for the moments has in the MPMM been simplified to only focus on the yaw of repose. The overturning moment has the biggest effect on projectile stability, as it is significantly larger than the other transverse moments [6]. Therefore, the MPMM neglects the other moments and only emphasizes on the overturning moments effect on the projectile stability. The yaw of repose is defined as

$$\boldsymbol{\alpha_R} = -\frac{2I_x p(\boldsymbol{v} \times \frac{d\boldsymbol{V}}{dt})}{\rho S d v^4 C_{M_\alpha}} \tag{13}$$

The angle of attack is approximated by

$$\alpha_t = \arcsin|\boldsymbol{\alpha_R}| \tag{14}$$

Unlike the 6-DOF model the projectile's current axial rotation speed is calculated separately

$$dp = \frac{\rho S d^2 v}{2I_x} p C_{lp} \tag{15}$$

2.4 Modelling software

The models were simulated in a software program called FLAMES. FLAMES provides both a global reference frame, called ECR which is fix in the center of earth, and a local body reference frame. The transformations matrixes needed to transform positions from one reference frame to another were easily implemented in the model by using predefined FLAMES transformation matrixes.

FLAMES supply the programmer with a vast library of functions that were very helpful. Atmospheric data can be uploaded to FLAMES by using its atmospheric model, which gives every projectile the either recorded weather or standard atmospheric data at its current

altitude. FLAMES uses a spherical earth model, which is necessary to acquire accurate results for greater distances due to the curvature of earth.

3 SYSTEM OVERVIEW OF A LIVE FIRE SCENARIO

To be able to fire at a target that cannot be seen by the gun crew, either because of the sheer distance or because of an obstacle in-between the howitzer and the target, an observer is needed. The observers report the position of the target and what kind of munition he finds suitable to use in order to neutralize the target. The Fire Direction Center (FDC) then calculates which gunpowder charge to use, elevation and azimuth angles the howitzer needs to use in order to hit the target, see Figure 4. Note that this is a broad overview, there exists variations from country to country, and also from weapon type what an artillery fire process looks like.

These calculations are either performed by using fire table manually, but nowadays it is more common with software that performs the needed calculations.

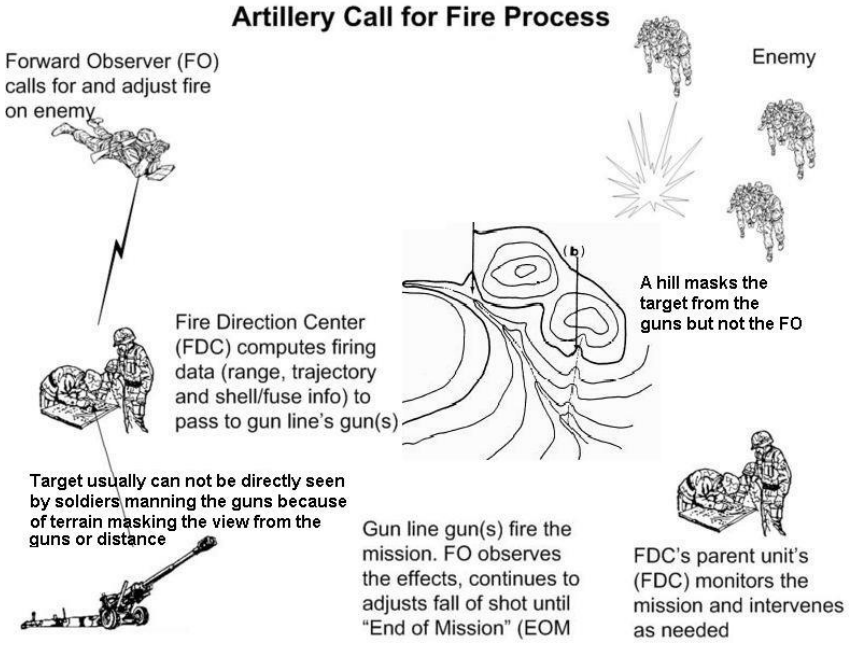

Figure 4. This figure shows how an artillery strike can be performed [18].

3.1 Conditions at firing site

When indirect fire (a term that distinguishes artillery from direct fire weapons such as rifles, as an artillery unit does often not have eye contact with their target) is deployed in practice some input data is needed in order to increase the probability of first round hit. Variations in wind and temperature have large effect on the trajectory of the projectile [10]. Therefore the weather needs to be measured continuously throughout the day in order to have correct atmospheric conditions. This is usually done by measuring the wind, temperature and pressure at different altitudes multiple times a day with a weather balloon. The Swedish armed forces require the weather to be measured at a maximum 30 km from the intended maximum altitude of the projectile's trajectory [10].

Artillery projectiles are usually quite precise in drift, but less precise in length. This is to large extent due to the unique conditions of the internal ballistics for each projectile. A saying in the Swedish artillery is that you can never fire the same projectile twice, meaning that every shot fired is unique and it cannot be replicated. How the gunpowder ignites has a large effect on the muzzle velocity of the projectile, and therefore the precision in length suffers. To better predict the muzzle velocity of next round, a v0 radar can be mounted on each howitzer. The v0 radar measures the muzzle velocity and can thereby give a better prediction of the next rounds initial velocity.

The position of the howitzer is usually measured with either an inertial navigation unit (INU), that uses a gyroscope to measure angular rate, in combination with an accelerometer that calculates linear acceleration [11]. A problem with an INU is that the position error diverges with time, as the new position is integrated from acceleration to distance traveled and added to the previous position. GPS (Global Positioning System) can also be used to determine position; however inertial navigation units are often favored by the armed forces, mainly because a GPS signal might not always be received but also because an INU does not receive any external signal which makes it harder to detect than for example a GPS supported positioning system. Combinations of inertial navigation units and GPS are also in use today, for example in the Swedish howitzer Archer.

As each projectile is a unique individual, they all differ slightly from one another. They differ in mass and the location of mass center, and each projectile can therefore be weighed individually to increase the accuracy. A heavier projectile will travel further than a lighter projectile, provided that both projectiles have the same muzzle velocity. The location of the projectile's center of mass is usually ignored because it is more difficult to locate.

4 IMPLEMENTED MODEL

The previously mentioned MPMM and 6-DOF models were applied to a real fire scenario performed by Artilleriets stridsskola (ArtSS) located in Boden. This section describes how the models were implemented to test the accuracy of the models compared to real fire data. Assumed uncertainties are estimated by an employee at BAE system at Karlskoga. The Swedish army uses the unit angular mil for angles instead of degrees; therefore all angular mil angles had to be converted to degrees because that is the unit that the model uses. A mil is defined as 6400 mils/revolution [12]. A 6-DOF model screenshot from the 3D view available in FLAMES is shown in Figure 5, where all forces and moments that are used in the 6-DOF calculations are visible. All vector lengths have been normalized in this 3D view.

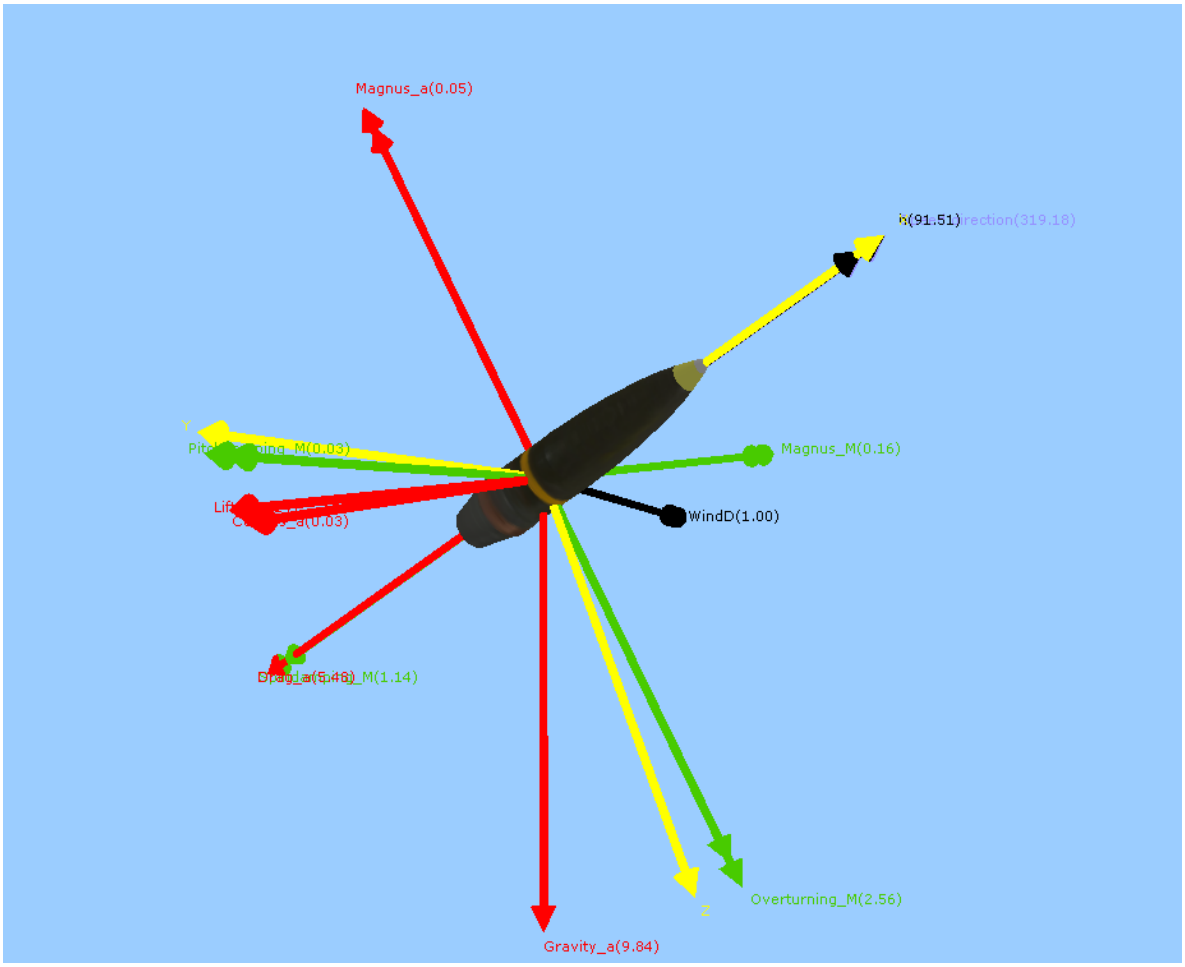

Figure 5. This screenshot from FLAMES that shows the projectile during flight. The green vectors are the moments, the red the forces, black wind and angular momentum, and yellow is the projectiles body coordinate system.

Figure 6 shows the 2D view in FLAMES, when viewing the target area. The numbers next to the hits indicate the targets speed and altitude, since they are stationary and on the ground level all numbers are zeros. This screenshot was taken during a simulated fire series later referenced to in the results section.

Figure 6. Screenshot from FLAMES showing the target (named goal, located in the upper half of the lake) the actual hits from the fire data and simulated hits (the craters to the right).

All uncertainties and deviations values mentioned later in this chapter were assumed maximum deviation levels, meaning they were assigned a certain numerical value that the error were not allowed to be larger than. These maximum deviation levels are the same numerical values as the assumed uncertainties. The error was then randomly generated using predefined FLAMES functions during the simulation using a Gaussian distribution. The standard deviation was set to half of the maximum deviation levels.

4.1 Integration method

The Adam-Bashforth 5^{th} order integration method was used. It is easy to implement because it does not use estimation of future derivatives, but four previous values [13]. Appropriate time step was chosen empirically and is static during the simulation. Runge-Kutta 4^{th} order integration method is the most common in the field of exterior ballistics [6], but was not implemented in this thesis due to complexity reasons. Runge-Kutta 4^{th} order need approximations of the derivatives at the next time step, and was therefore disregarded in this thesis.

4.2 Time step

Suitable time step for the MPMM is set to 0.01s [5]. The time step for the 6-DOF model was decided by running multiple simulations and analyzing the results. The precision for the 6-DOF model is relatively good whenever the projectile is stable, because when the time step is too large the projectile will start to tumble. When the time step is small enough to generate a stable projectile, the precision is <1 m. Figure 7 shows the time step as the x axis and relative precision on the y-axis. The relative precision was calculated by dividing all results with the results from the smallest time step, which was $10^{-4}s$. Smaller time step could not be used because of the very long simulation times required for such time steps. In order to quantify the precision versus Time step, a term named relative precision is introduced. All values are compared to the value that is arguably the most precise, i.e. the one with the shortest time step. The other values, from other time steps, are then compared to the most precise value. The relative precision is a ratio between the most precise result and the result with the currently used time step. From Figure 7 conclusions can be made that the relative precision is to some extent independent of the time step, as long as the time step is smaller than 10^-3 seconds. With values larger than 10^-3 seconds the relative precision is far from 1.

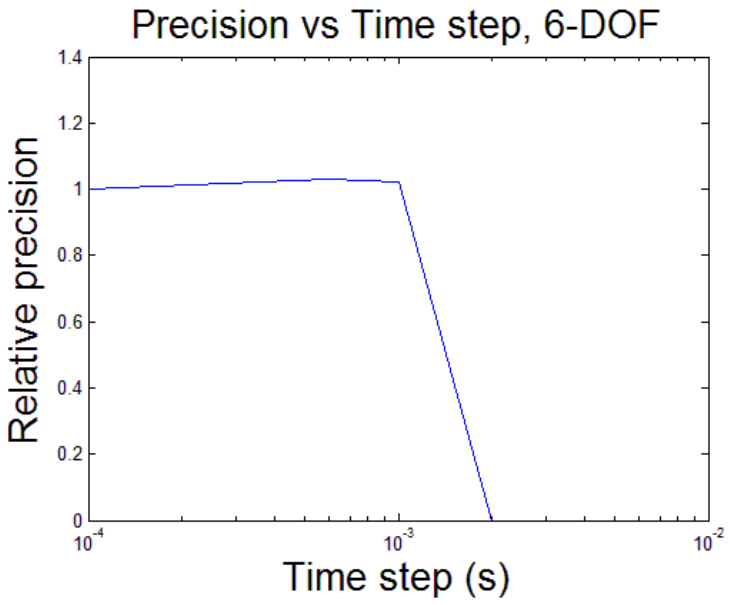

Figure 7. Relative precision vs time step. Time step smaller than 10^{-4} caused very long simulation times, and time step bigger than 10^{-3} resulted in an unstable trajectory.

4.3 Azimuth and elevation deviation

This deviation comes from hydraulic sensors and uncertainties in the bearing from INS. The deviations were assumed to be maximum 1 angular mil [14].

4.4 Aerodynamic data

The coefficients for the m/sgr77 projectiles were supplied by ArtSS, most coefficients are functions of the angle of attack and Mach number. The Mach number is defined by

$$Mach = \frac{v}{\sqrt{\frac{1.4P}{\rho}}} \tag{16}$$

where P is the current pressure ρ the current density of the air and v the total speed. The coefficients were delivered originally in table format, and they were transformed into splines using MATLAB.

4.5 Positioning system

The positioning system of the howitzer uses an INU (*Inertial navigation Unit*). Uncertainties will be assumed to be maximum 25 m horizontally and 10 m vertically [14]. As a clarification horizontal refers to the ground plane and vertical upwards towards the sky.

4.6 V0 radar

Each howitzer had an initial velocity (v0) radar mounted to measure the muzzle velocity of every fired shell. The v0 radar inaccuracy is assumed to be 0.5 m/s [14].

4.7 Projectile

The projectile itself varies in weight and mass symmetry. Every projectile has a unique weight and location of center of mass. This thesis will neglect mass asymmetry but considers mass variations. During normal circumstances, the manufacturer of the projectiles labels them in different weight groups, in order to achieve higher accuracy. With these labels the mass uncertainty is +/- 0.25kg. However, during the live fire scenario data that is used in this thesis, the projectiles were weighed individually with a higher degree of certainty. Therefore the uncertainty of +/- 0.25kg will only be used during the precision part of this thesis. Constant projectile parameters are defined in table 1.

Table 1. The data in this table is constant for the projectile during all simulations.

Diameter (m)	I_y (Kgm^2)	I_x (Kgm^2)	n (Calibers/turn)
0.155	1.3287	0.147	20

4.8 Atmospheric data

There are four different metrology weather splines for different times of the day, with timestamp 05:45, 08:33, 09:38, 10:00 and 13:00. The metrology was measured with a weather balloon during the respective timestamps, and was delivered in table format. The data included temperature, wind speed and wind direction in eight different altitudes. The altitudes range from 0m altitude above ground level to 4000 m above ground level. Pressure was not measured for an unknown reason, possibly because of a faulty sensor on the weather balloon, and therefore estimated internally in FLAMES with temperature as input. FLAMES uses a standard atmospheric model (U.S Standard Atmosphere 1976) if no external atmosphere is imported. The standard atmospheric data assumes no wind.

4.9 Summary of uncertainties table

Table 2. This table summarizes all assumed uncertainties used later in this paper, specifically in section 6.8.

Uncertainties variable	Maximum assumed variation
V0 radar	+/- 0.5 m/s
INU Position	25 m horizontally, 10 m vertically
Projectile mass	+/- 0.25 kg
Elevation and azimuth angles	+/- 1 mils

4.10 Live fire data

The live fire data comes from a training exercise in Boden in 2001. The rounds were fired by an FH77, recently retired from the Swedish artillery. Its replacement, the FH77D, usually referred to as Archer, is a highly modified version of the earlier mentioned howitzer.

The data received from ArtSS were atmospheric data, position of the howitzers, targets position, position of the real hits, angle of azimuth/elevation, muzzle velocity and projectile mass. The fire data consists of a total of 7 fire series, consisting of 2-5 rounds fired/series. The series 1, 2, and 3 (will combined be referenced to as scenario 1 later in the paper) are fired at the same target, and series 4, 5, 6, and 7 (reference to as scenario 2) are fired at another target. The fire data coordinates were transformed from RT90 coordinates used by the Swedish Armed Forces to standard longitude and latitude coordinates that FLAMES use. The transformations were performed using an online tool [15].

5 VERIFICATION OF THE 6-DOF MODEL

In this section the 6-DOF model was compared to a fire data table from an FH77B howitzer. The verification was performed by designating an initial velocity and elevation and then input the same parameters into the model. The length and drift from the fire table for those inputs were then compared to the models output for the same inputs. As mentioned earlier in the limitations section, the 6-DOF model and the fire table use different atmospheric models, both assumes no wind. The fire table uses angular mils to measure angles, and that unit is therefore used in table 3. The fire table did not have tabular values for the same elevation angles for different initial velocities, therefore the value that was closest to the elevation 540 mils was chosen. Since the fire table did not take Coriolis Effect into account, it was removed from the 6-DOF model during the verification stage. During the verification a standardized atmospheric model for temperature used by the Swedish armed forces was used, however no standardized atmospheric model for pressure was available, therefore US standard was applied.

5.1 Distance and drift

This section compares distance traveled and drift for the 6-DOF model and fire table data. Positive drift is defined as to the right when viewing downrange (from the howitzer towards the target), perpendicular to the trajectory.

Table 3. This table shows length and drift for the fire table and 6-DOF model at different initial velocities

Initial Velocity (m/s)	Elevation (mils)	Length(m) (from table)	Length (m) (6-DOF)	Drift (m) (from table)	Drift (m) (6-DOF)
345	560	8400	8445	107	84
400	562	9700	9737	137	100
473	555	11400	11427	179	120
559	540	13600	13611	239	154
658	558	16200	16172	309	200

Table 4. This table shows the error in length and drift in percent at different initial velocities.

Initial velocity	Error in length (%)	Error in drift (%)
345	0.5%	21%
400	0.4%	27%
473	0.2%	33%
559	0.1%	36%
658	0.2%	35%

Table 4 shows that the error in drift grows with the firing distance, and the error in length decreases with increased firing distance. The drift from the 6-DOF model is consequently smaller than the fire table values.

5.2 Projectile stability

In order for a projectile to be stable during flight, it has to fulfill both a gyroscopic stability criterion and a dynamic stability criterion. The two following equations (17) and (18) describe the gyroscopic and dynamic stability criterion respectively, slightly modified from McCoy's work [6].

$$S_g = \frac{{I_x}^2 p^2}{2\rho I_y S d v^2 C_{M_\alpha}} \tag{17}$$

$$S_d = \frac{2(C_{L_\alpha} + \frac{md^2}{I_x} C_{M_{p\alpha}})}{C_{L_\alpha} - C_D - \frac{md^2}{I_y}(C_M)} \tag{17}$$

In order for the projectile to be stable the conditions $S_g > 1$ and $2 > S_d > 0$ must be fulfilled. Figures 8 and 9 show S_g and S_d during the first verification test, which had an initial velocity of 345 m/s. The S_d and S_g parameters are recorded and monitored in all test cases performed but only shown in this section. Beta and alpha angles are referred to in future sections instead when discussing projectile stability. Figure 10 illustrates the beta and alpha angles when the projectile is stable, and will be used as a reference of stability in future sections.

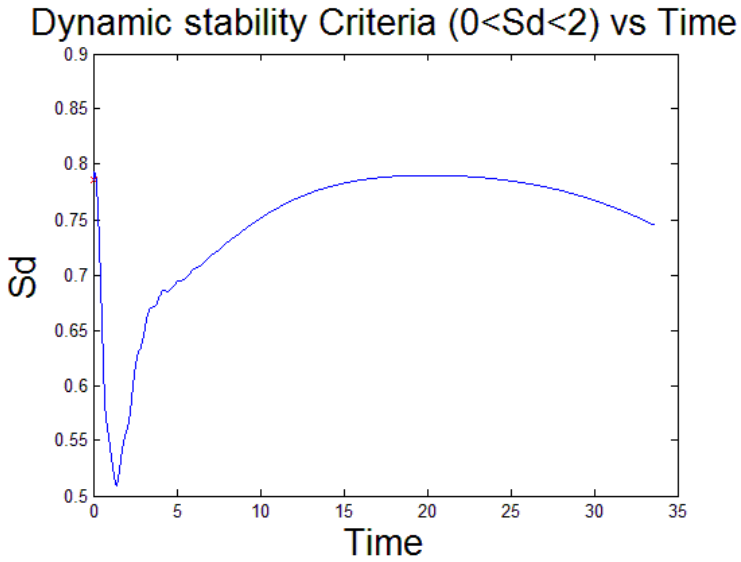

Figure 8. The dynamic stability criterion is fulfilled during the entire trajectory.

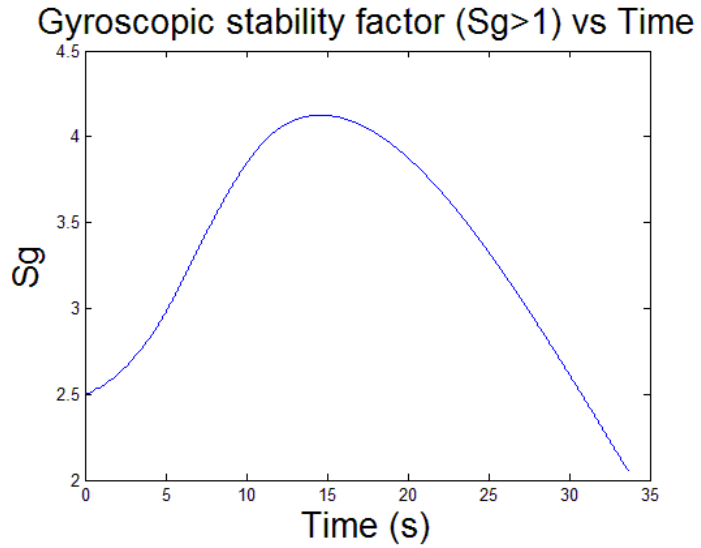

Figure 9. The gyroscopic stability criterion is fulfilled in every point along the trajectory.

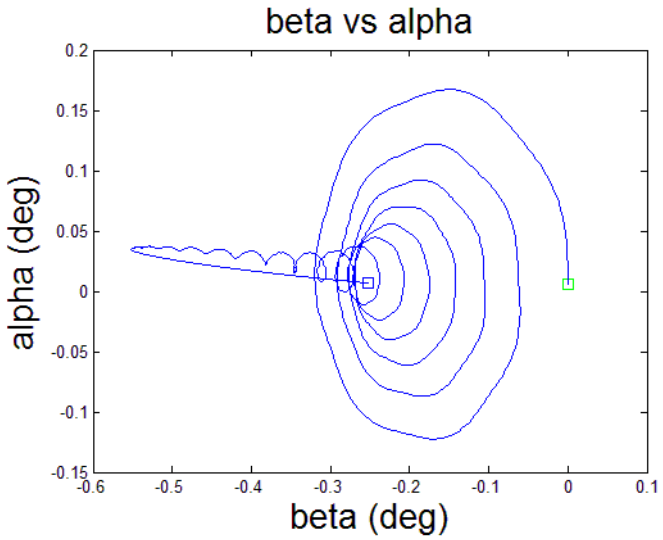

Figure 10. This Figure illustrates the behavior of the beta and alpha angles when the projectile is stable, i.e. when the stability criterions are fulfilled.

Figure 8 and 9 shows that both stability criterions are fulfilled in every point along the trajectory, thus the projectile can be assumed to be stable. Figure 10 is not part of the stability criterion, it is merely included to show the reader an example of what an alpha vs beta plot can look like when the stability criterions are fulfilled. Remember that alpha and beta are pitch and yaw components of the angle of attack, meaning that if alpha and beta are increasing

the projectile's nose would end up pointing in a different direction than towards the trajectory. If that would happen, the projectile would be unstable, and would start to tumble through the air in an uncontrolled matter. The beta and alpha angles are defined as viewed from the projectile's nose, i.e. negative beta angles means that the projectile has a positive yaw (to the right when viewed from the base of the projectile). Figure 10 shows a circular motion initially with decreasing amplitude, indicating stability.

6 RESULTS

In this section results from the 6-DOF model and MPMM are shown. Data from the models such as angle of attack, speed, attitude and distance were continuously logged during the trajectory, and were afterwards processed in MATLAB.

6.1 6-DOF vs MPMM simulation hits

The fire series 1, 2, and 3 were all aimed at the same target. In these test series no uncertainties were assumed. The graphs coordinates system originates in the target location, and the coordinate system has been transformed to be aligned with a tangent from the howitzer to the target. The measured atmospheric conditions with the closest timestamp were chosen. The target is located in the center, with coordinate (0, 0). The approximate firing distance was about 15 km.

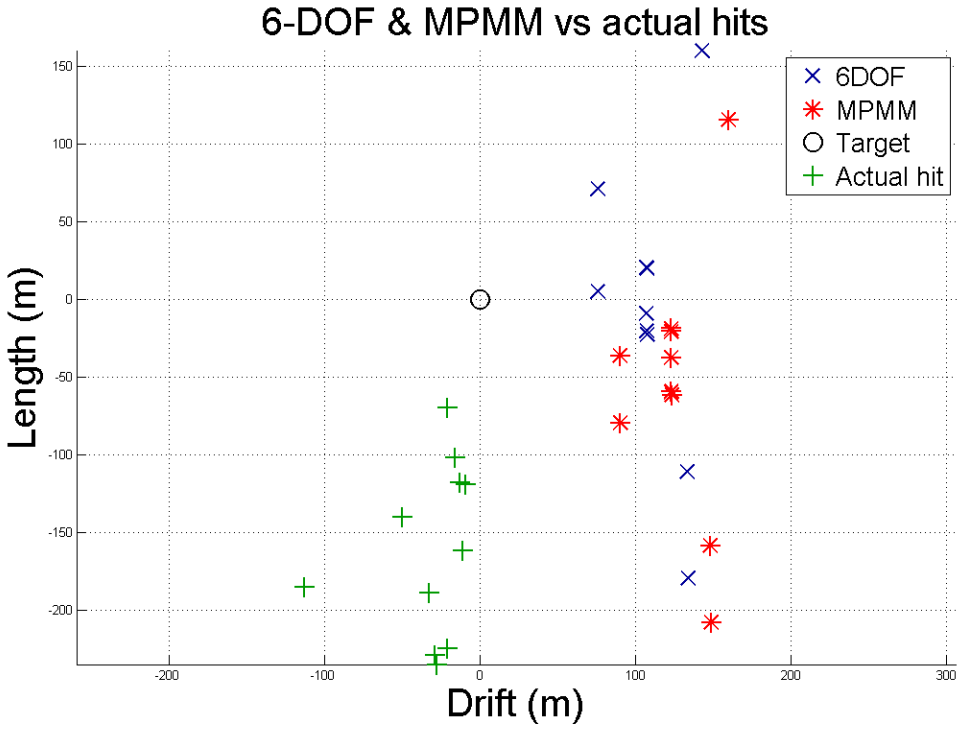

Figure 11. This plot shows the results from scenario 1. All simulated projectiles hits to the right of both the target point and actual data points.

The remaining projectiles were simulated in scenario 2, available in Figure 12. The projectiles in scenario 2 were fired later during the day, with different atmospheric conditions being used. The firing distance was shorter, approximately 12 km.

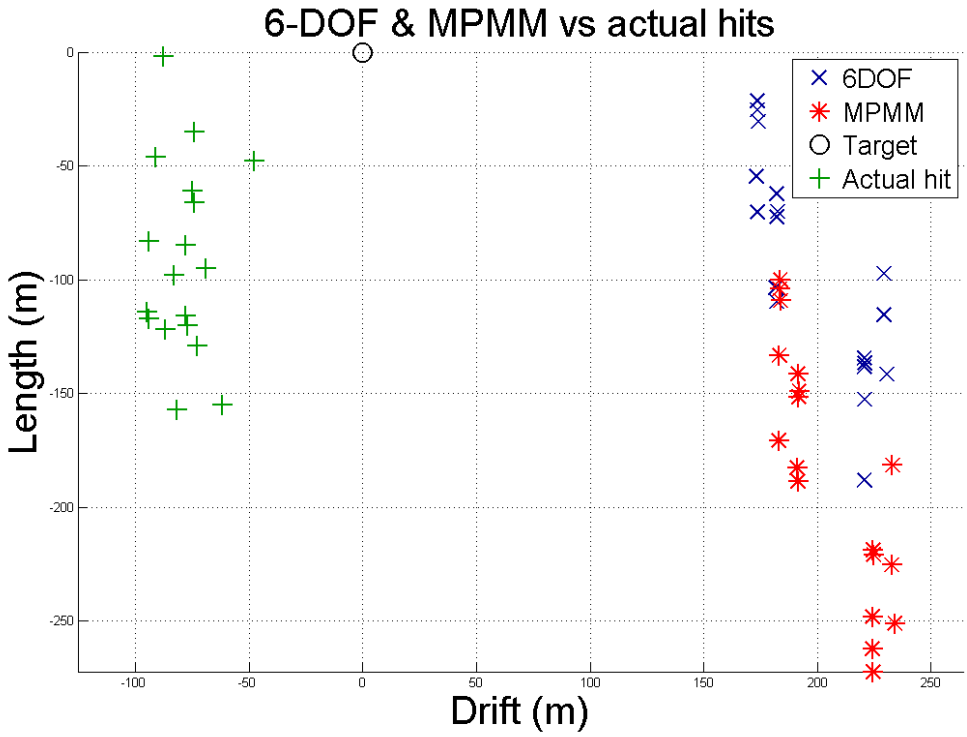

Figure 12. Results from scenario 2, the simulated projectiles are concentrated to the right hand side of the plot.

6.2 6-DOF vs MPMM simulation time

FLAMES is not a simulation optimization tool such as Simulink or many others, therefore it lacks functionality to easily compare memory usage and precise simulation time. Since FLAMES has a 2D and 3D views of the simulation environment, some computer power is needed for such presentations. In any case, the simulation time was clocked for comparison reasons between the 6-DOF model and the MPMM model, by measuring the time it takes from launch to impact at a specific range, at highest simulation speed. The range was 15 km, and the 6-DOF took 41 seconds, and the MPMM 15 seconds.

6.3 Mean distance 6-DOF and MPMM to target

In this section the mean distance between the actual hits and the MPMM and 6-DOF model are compared. Statistical values such as maximum and minimum difference will be presented, as well as standard deviation, variation and mean distance.

The results from scenario 1 & 2 from section 6.1 are presented below, in Figures 13 & 14 and in Tables 5 & 6.

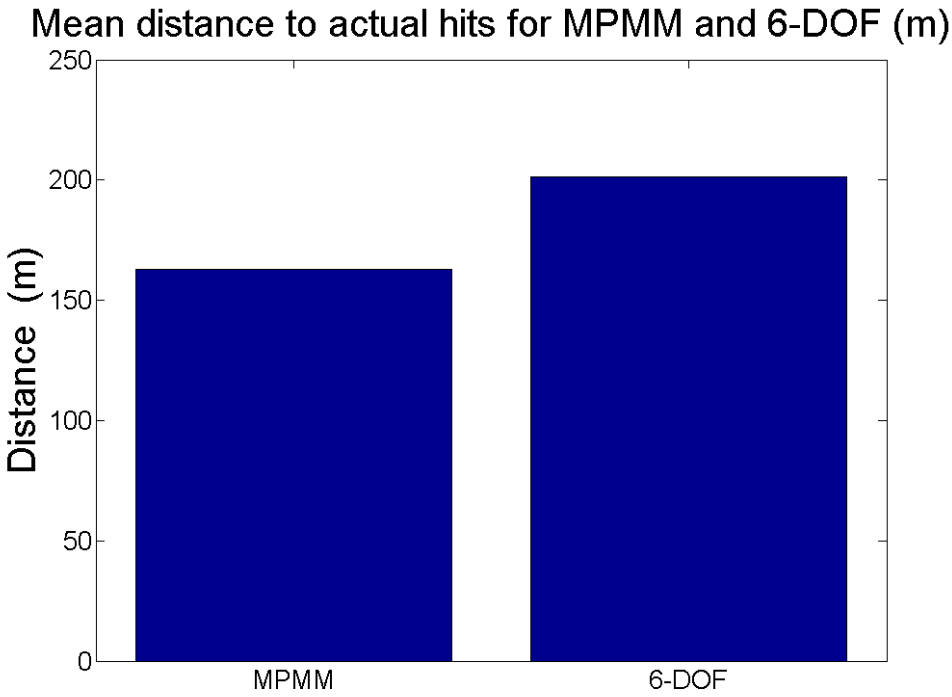

Figur 13. Mean distance between the simulated hits and the actual hits from scenario 1..

In scenario 1 the 6-DOF model performed worse than the MPMM. In the table below the statistical data is presented from scenario 1, the mean distance between the models and the actual hit can be seen in Figure 13.

Table 5. The statistical data from scenario 1.

Scenario1	**6-DOF**	**MPMM**
Maximum (m)	424	341
Minimum (m)	153	131
Standard deviation	85	68.7
Variance	7237	4725

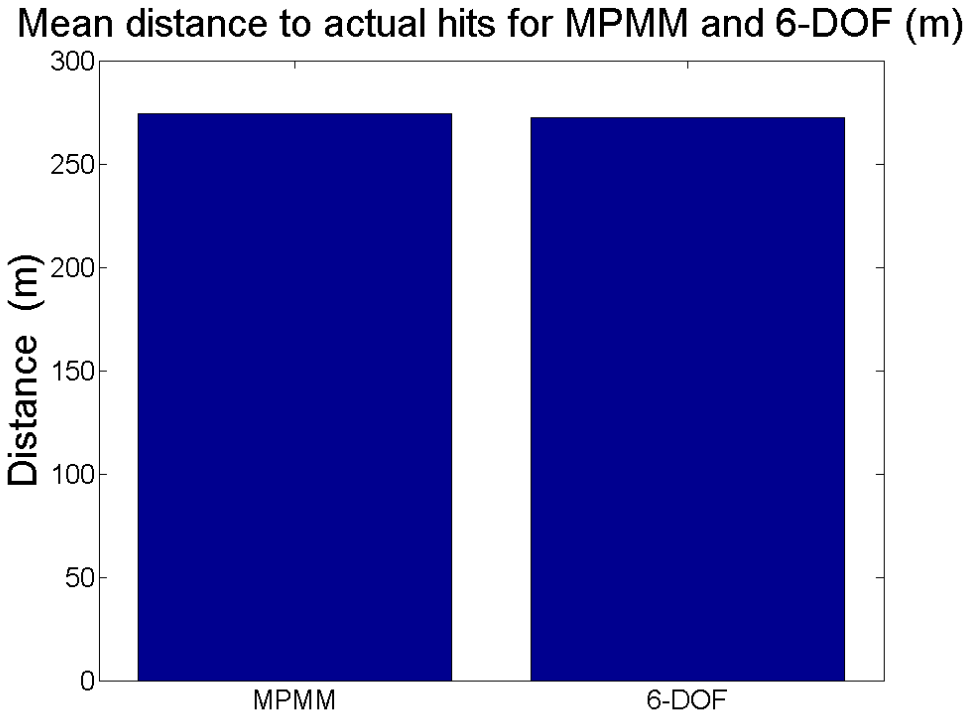

Figur 14. Mean distance between the simulated hits and the actual hits from scenario 2

Table 6. The statistical data from scenario 2.

Scenario2	**6-DOF**	**MPMM**
Maximum (m)	337	337
Minimum (m)	251	171
Standard deviation	28	57
Variance	809	3285

6.4 Angle of attack, 6-DOF model

These graphs show the behavior of the angle of attack during flight, from leaving the barrel to impact. Figures 15 and 17 were simulated with measured atmospheric conditions measured at 8:33, while Figures 16, 18 were simulated with identical initial conditions except using standardized atmospheric conditions i.e. no wind instead of measured. These simulations were performed with an elevation angle of 37° and an initial velocity of 577 m/s. In Figure 17 and 18 the initial values of beta and alpha were (0, 0), indicated by a green box in the Figures.

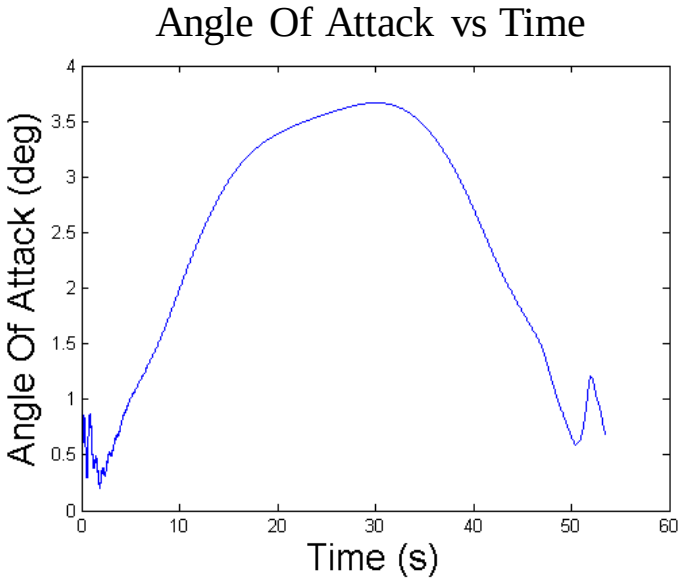

Figure 15. Angle of attack for a 6-DOF simulation with measured atmospheric conditions

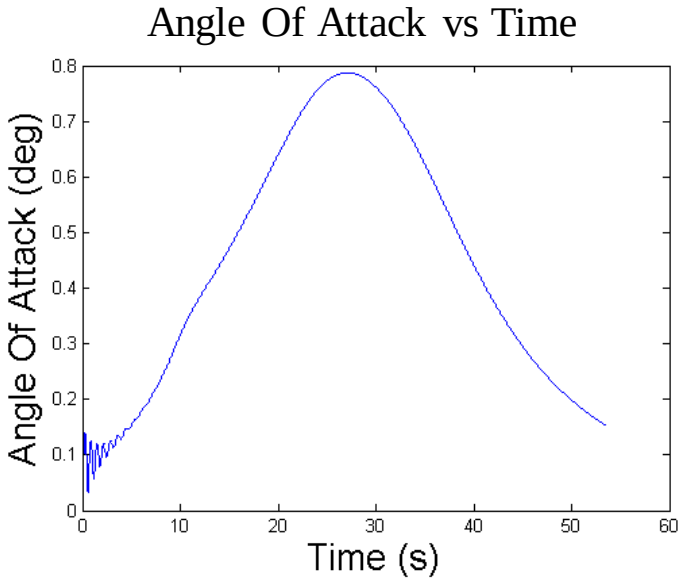

Figure 16. Angle of attack for a 6-DOF simulation with measured atmospheric conditions

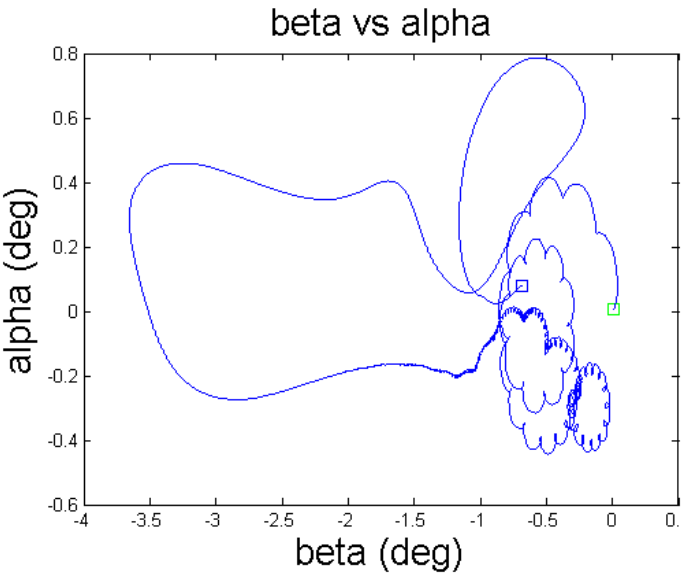

Figure 17. Beta vs Alpha angles with measured atmospheric conditions, from the 6-DOF model.

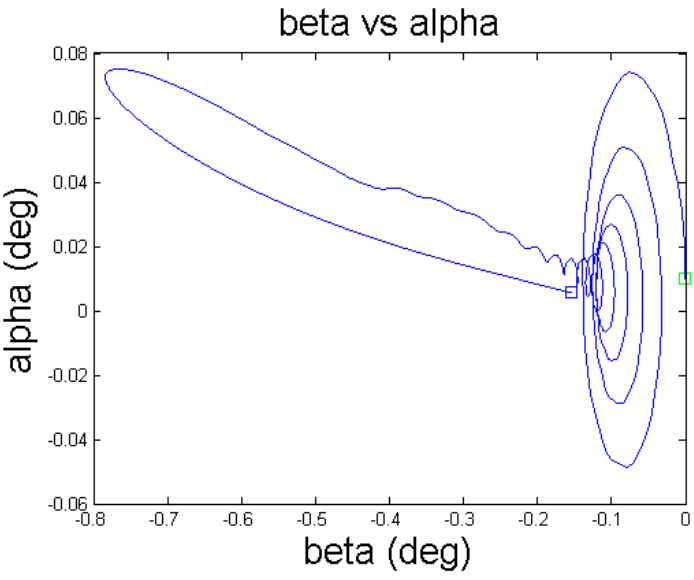

Figure 18. Beta vs Alpha angles with standardized atmospheric conditions, from the 6-DOF model.

The winds effect of the beta and alpha angles are clearly visible from Figures 17 and 18, as the only difference in the settings was different atmospheric conditions.

6.5 Angle of attack, MPMM

The following graphs show angle of attack of a projectile fired in series 1, performed with an elevation angle of 37° and an initial velocity of 577 m/s. Note that beta and alpha angles are not available for MPMM simulations, and could therefore not be included. The difference between Figures 19 and 20 is minimal, indicating that the effect on the angle of attack from the wind is minimal when using the MPMM.

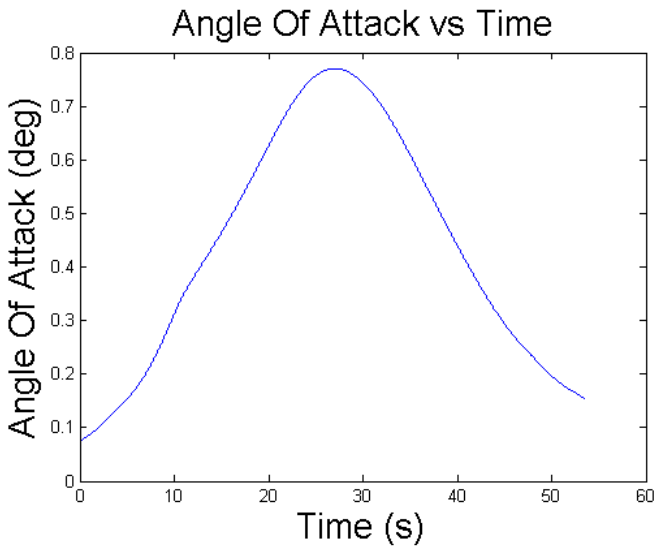

Figure 19. MPMM simulation with measured atmospheric conditions

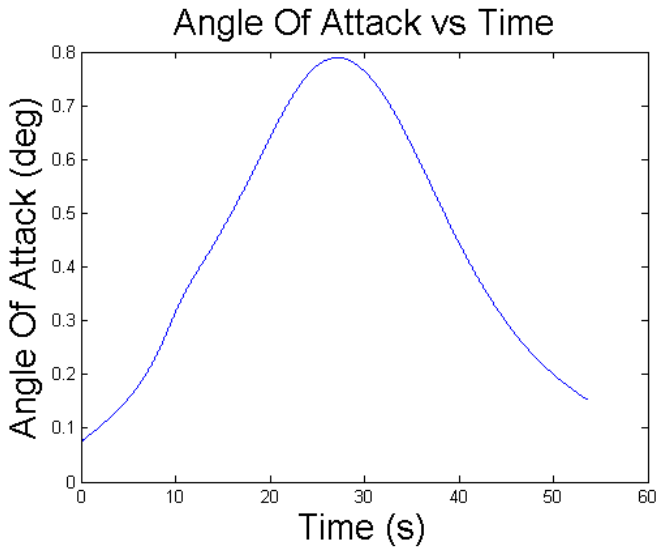

Figure 20. MPMM simulation with standardized atmospheric conditions

6.6 High elevation simulation, 60° elevation

In Sections 6.6 and 6.7 the MPMM and 6-DOF models performance was tested with a high elevation angle. The initial velocities for both sections were set to 577 m/s for both test cases. Since the projectiles maximum altitude was above 4000 m above ground level measured atmospheric conditions could not be used, as the simulated projectiles traveled well above 4000m. Figures 21 and 22 are similair, indicating that there is little difference betweem the MPMM and the 6-DOF model at 60° elevation angle.

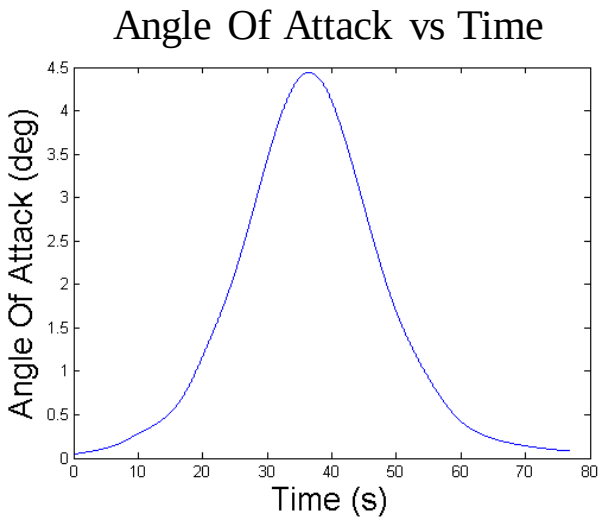

Figure 21. Angle of attack for MPMM with 60° elevation

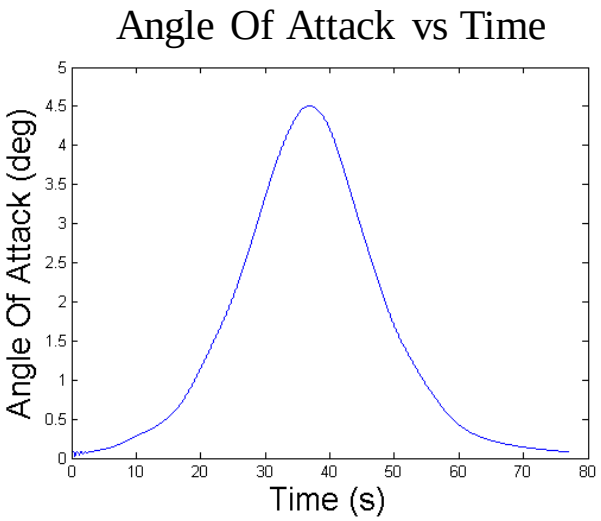

Figure 22. Angle of attack for 6-DOF model with 60° elevation

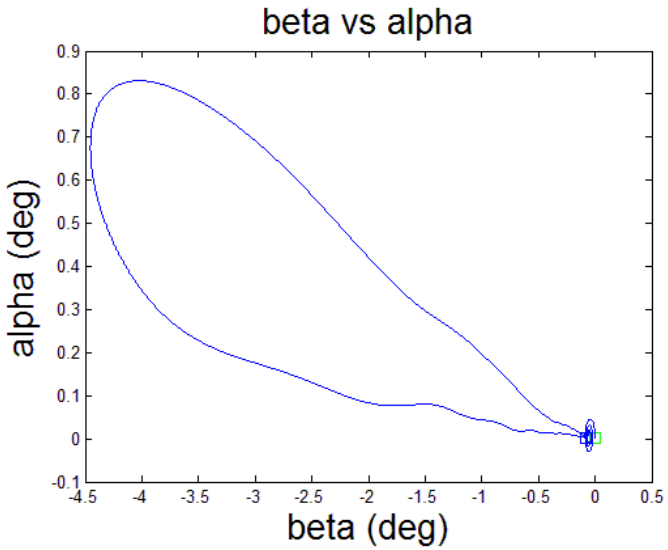

Figure 23. Alpha vs beta for the 6-DOF model with 60° elevation. This figure shows initial similarities with Figure 18; however the yaw increase (beta angle) is significantly larger.

6.7 High elevation simulation, 70° elevation

This section uses identical initial values as section 6.6 but with 70° elevation. The difference between Figure 24 and 25 is apparent; the angle of attack in Figure 25 is significantly different at the end phase of the trajectory compared to Figure 24.

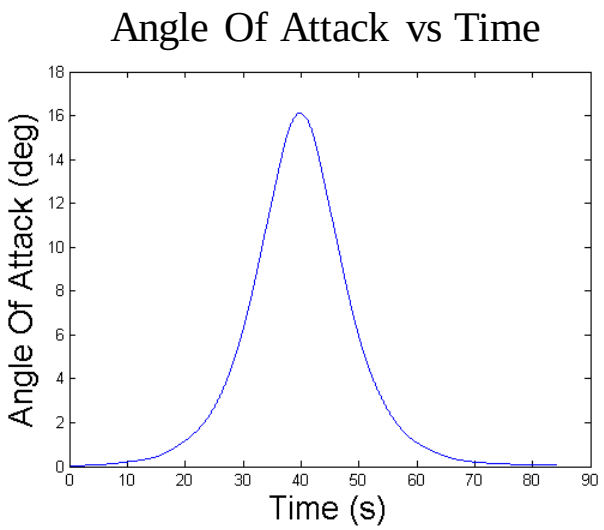

Figure 24. Angle of attack for MPMM model with 70° elevation

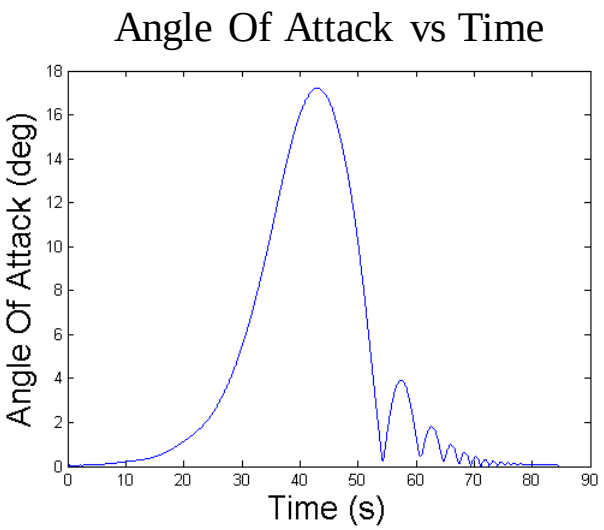

Figure 25. Angle of attack for the 6-DOF model with 70° elevation

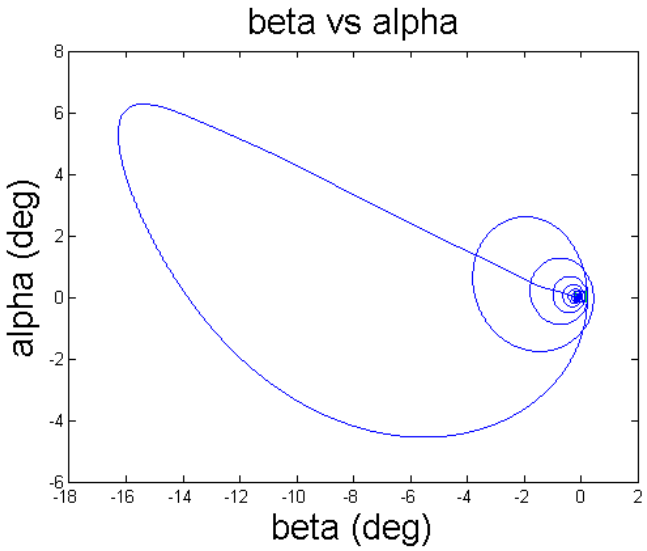

Figure 26. Alpha vs beta for 6-DOF model with 70° elevation. The model starts with a large increasing beta angle, and at the end phase starts to spiral with decreasing amplitude towards a stable state close to origin.

6.8 Simulation with uncertainties compared to real data

In this fire series the 6-DOF model fired with uncertainties. 55 projectiles were simulated during standardized atmospheric conditions, with uncertainties according to section 4.9. The initial velocities mean values was 467 m/s and elevation 37°. Figures 27 and 28 show results from simulated projectiles that traveled approximately 15 km. Each red dot illustrates a 6-DOF model hit, and the ellipses encircle 90% and 50% of all simulated hits. The bar graphs next to and below and left to the plot describes the distribution of the hits, with the majority hitting close to origin. The y-axis shows the length in meters from the average length, and the x-axis shows the drift in meters from the average drift.

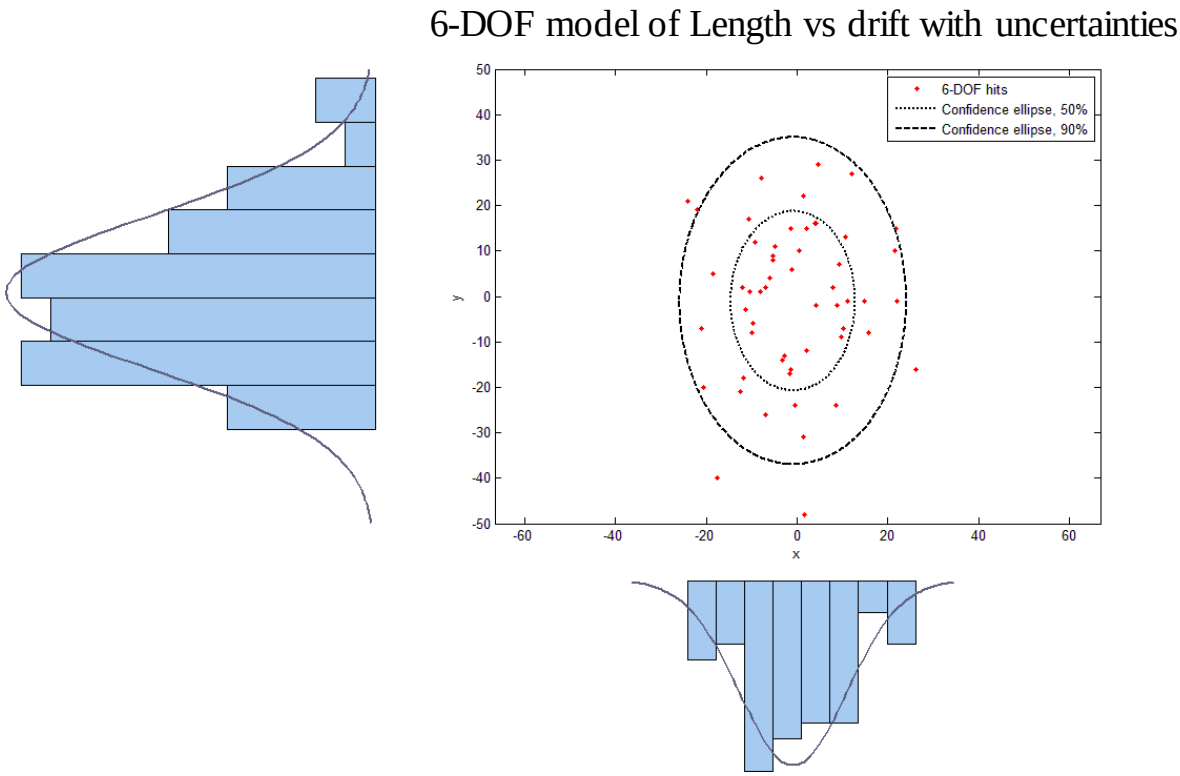

Figure 27. Simulated 6-DOF model hits with 2 confidence ellipses.

Confidence ellipses were also applied to actual fire data, from scenario 2. Figure 28 shows that the precision of the real data hits is less than in Figure 27, because the ellipses in Figure 28 are longer (in the y-axis direction) but approximately the same width. The red dots represent actual hits from the fire data, and they were fired from different howitzers with slightly different angle of elevation and azimuth. The y-axis and x-axis are defined as in Figure 27.

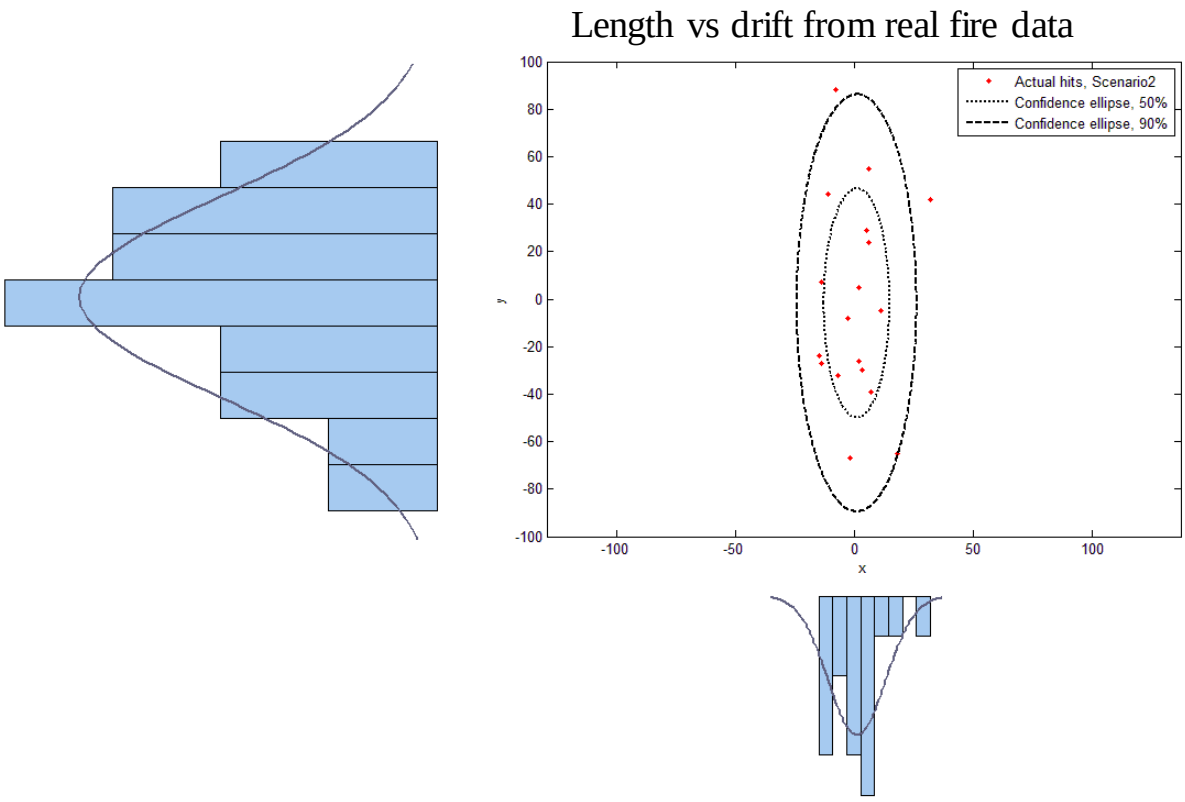

Figure 28. Actual hits from scenario 2 with confidence ellipses

7 DISCUSSION

In this section the results from the previous section is discussed, suggesting strengths and drawbacks of the different models.

7.1 Verification of 6-DOF model

The verification in section 5 showed that the error in length is significantly smaller than the error in drift. That the error in length is small is unsurprising, big factors on length such as drag is quite simple to model, a model with few degrees of freedom could perform length calculations with reasonable accuracy. The problematic parts are the angular moments that give yaw of repose and from there the drift effect. The results from the verification section show that the accuracy in drift has an upwards 35% error compared to fire tabular data. A plausible explanation could be that it is because different atmospheric models were being used, and the U.S standard atmospheric model might give unrealistic results for firing conditions in northern Sweden. Another plausible reason for this rather large error is that the lift force coefficient is incorrect and may therefore introduce a drift error. This is due to the fact that the lift force is the main force effecting for the drift.

Section 5.2 shows that the projectile is stable during the trajectory and this can be confirmed by looking at alpha vs beta angles. The projectile becomes unstable when the alpha and beta angles increase indefinitely in amplitude, which is not the case according to Figure 10.

7.2 6-DOF vs MPMM

In scenario 1, Figure 13, the MPMM has smaller mean distance to actual hit than the 6-DOF. Both models have drifted approximately the same length, but the 6-DOF model has traveled further than both the actual hits and the MPMM model. In scenario 2 the mean distance to actual hits are equal for both models. All simulated projectiles hit at a minimum of 131m from the actual target, and at a maximum of 424 m. The standard deviation was between 28 and 85, implicating that the deviation from the mean is approximately between 85 to 28 meters. All simulation hits to the right of the target, both the MPMM and the 6-DOF model, and all real hits to the left of the target. This could be explained by either wrong atmospheric condition, the wind was blowing from the east that day and it is a possibility that the wind was stronger than measured. Another explanation, far more likely according to the author of this paper, is that there is an error in the azimuth angle. As discussed earlier, in section 2.1, artillery projectiles with a right hand twist tend to drift to the right because the yaw of repose is pointing to the right of the trajectory. This is confirmed in the verification section of this paper, as both the model and fire table data shows that the drift is to the right. Therefore it can be expected that the projectiles hit to the right of the target, if the howitzer is aimed directly towards it. In reality this drift is offset by aiming to the left of the target and this offset could be missing, Figure 6 shows that the howitzer is aiming to the right of the target which the author finds this unlikely in reality. The verification section also clearly shows that the models

drift less than the fire table, and since the results from scenario 2 (Figure 12) shows that the modulated hits hit several hundred meters too far to the right, it can be concluded that it is not due to a drift error in the model. This statement is based on the assumption that the crosswind is not strong enough to completely neglect the side drift. High degrees of freedom models, such as the 6-DOF model, requires very accurate in-data, otherwise the results will not be what would be expected. McCoy states that the most common error from simulations is coefficients and other data with to low degree of accuracy, so called Garbage In-Garbage Out [6].

The angle of attack for the 6-DOF is highly weather dependent. The angle of attack in Figure 19 and 20 are different, both in appearance and in magnitude. In the MPMM the difference between Figures 23 and 24 are minimal. This is because the MPMM approximate the yaw of repose, and the effect of added wind to the angle of attack is missing. These result claims that when observing the angle of attack of a projectile during realistic atmospheric conditions the 6-DOF model is desirable. The beta and alpha components of the angle of attack shows the detailed movement of the projectile's nose during flight. Figure 22 shows expected behavior with a damped circular motion that reaches stability and thereafter the beta angle starts to increase. Figure 21 show the large effect of added wind, as the beta and alpha angle seems less stable than in Figure 22.

At 60° elevation angles, the results from Figures 25 and 26 show that the angle of attack for the MPMM corresponds well to the angle of attack of the 6-DOF model. The MPMM is a acceptable approximation at 60° elevation, because both models demonstrate similar behavior of the angle of attack. However, at 70° the angle of attack for the MPMM and the 6-DOF model is significantly different at the end phase of the trajectory. This corresponds well with results presented by McCoy [6]. McCoy states that the MPMM is not valid at high elevation angles, which Figures 28 and 29 indicates. The 6-DOF model in Figure 28 has an oscillating behavior of the angle of attack at the end phase, which the MPMM is lacking. Figures 27 and 30 shows that the behavior of the alpha and beta angles changes with increasing elevation. At 60° elevation the behavior of the angle of attack is quite normal, compared to Figure 24, but with larger amplitude. Figure 29 shows a circular motion towards the end phase, which has not been seen previously in this work, and that is a possible reason why the MPMM is no longer valid. Thus the 6-DOF model is preferable when examining the projectiles behavior when fired at an angle of elevation larger than 60°.

7.3 Dispersion due to uncertainties

Figure 31 shows that the dispersions of the simulated hits, 90% of all simulations will hit within an ellipse of roughly 50 m in width and 75 m in length. Compared to real fire data, that has a 90% ellipse of roughly 50 m x 180 m; it is a possibility that the current dispersion model is too precise in length. The precision in drift are approximately the same. This result is not surprising, as artillery shells indeed are less precise in length, because there are more factors attributing to the error in length (initial velocity, mass and elevation uncertainties), then in side drift (azimuth uncertainty as a possible big impact factor). Although, scenario 2 (Figure 28) is not ideal for such a comparison, because fire adjustments took place between the fire

series (change in elevation and azimuth between fire missions). When testing the precision of a weapon system no alterations should be made between each projectile, therefore Figure 28 might not be completely accurate, and more fire data is necessary to draw conclusions from the real fire data.

In this work the main focus of uncertainties relied on sensor errors, which is not always relevant. For example in initial velocity the v0 radar has been assumed to have an approximate error of 0.5 m/s. While that might be an assumption that corresponds well to reality, it is not the same thing as saying that the initial velocity will deviate by maximum 0.5 m/s. What that assumption does say is that all recorded initial velocities can deviate by an assumed maximum of 0.5 m/s. A better way to simulate the initial velocity uncertainties would possibly give results that corresponds better to the reality.

7.4 Further work

This thesis provides an understanding of the differences of the MPMM and the 6-DOF model, but more reliable fire data is needed to compare and validate the existing 6-DOF model with the real world. More fire data is also needed for further work with the uncertainties for a weapon system, because with more data it would be possible to determine uncertainties more accurately then what has been assumed in this thesis. For example the muzzle velocity needs to be better estimated, as section 6.8 indicates.

Investigations in different integration methods, such as the Runge-Kutta fourth order, could also increase the precision and speed of future simulations.

Since the lift force coefficient is a possible reason for the drift error, it could be interesting to investigate. It could be estimated by empirical testing, by manually changing the lift force coefficient until the drift corresponds to the data from the fire table.

8 CONCLUSIONS

Simulations comparing the MPMM and the 6-DOF model showed that the 6-DOF model performed worse at a real scenario; plausibly due to in data of to low accuracy. This thesis also demonstrates certain scenarios where the MPMM is unsuitable, such as at high elevation angle and when the angle of attack is being examined when there is a wind present. The verification of the 6-DOF model showed a significant error in drift compared to a fire table for FH77B, which might come from either wrong coefficient values or wrong atmospheric model being used. The results from the added uncertainties to the model concluded that the 6-DOF model had similar precision in drift as the real data, but in length it did not correlate as well. This is possibly due to wrong assumptions in initial velocity uncertainties.

9 BIBLIOGRAPHY

[1] M. Cartwright, "www.ancient.eu," 2 February 2014. [Online]. Available: http://www.ancient.eu/article/649/. [Accessed 26 May 2015].

[2] H. Whipps, "www.livescience.com," 6 April 2008. [Online]. Available: http://www.livescience.com/7476-gunpowder-changed-world.html. [Accessed 26 May 2015].

[3] NATO Standardization Agency (NSA), "Glossary of Terms and Definitions," 2008.

[4] F. Fresconi, G. Cooper, I. Celmis, J. DeSpirito and M. Costello, "Flight mechanics of a novel guided spin-stabilized projectile concept," U.S. Army Research Laboratory, Maryland, USA, 2010.

[5] O. Nordgren, "Development and Evaluation of a Modified Point-Mass Trajectory Model using Fire Data," KTH, Stockholm, 2014.

[6] R. L. McCoy, Modern Exterior Ballistics, Surrey: Schiffer Publishing Ltd, 2012.

[7] Ternion, ”FLAMES,” [Online]. Available: http://www.ternion.com/. [Använd 3 Juni 2015].

[8] R. Kent, "Notes on a Theory of Spinning Shell," Aberdeen Proving Ground, Maryland, 1954.

[9] D. E. C. &. S. S. Jacobsen, Ballistics, Theory and Design of Guns and Ammunition, Taylor & Framcis Group, LLC, 2014.

[10] Försvarsmakten och Försvarsmedia, KA Artlära, Värnamo: AB Fälths Tryckeri, 1994.

[11] S. H. Stovall, "Basic Inertial Navigation," Naval Air Warfare Center Weapons Division, China Lake, California, 1997.

[12] [Online]. Available: http://www.thefreedictionary.com/mil. [Accessed 3 September 2015].

[13] D. Allerton, Principles of Flight Simulation, J Wiley & Sons Ltd, 2009.

[14] M. Eliasson, Interviewee, *Email conversation regarding an artillery systems uncertainties.* [Interview]. 24 Februari 2015.

[15] A. Andreasson, "Konvertering SWEREF99/RT90/WGS84," [Online]. Available: http://latlong.mellifica.se/. [Accessed 28 May 2015].

[16] [Online]. Available: http://thearmsguide.com/5341/long-range-shooting-external-ballistics-bullet-shape/. [Accessed 3 September 2015].

[17] [Online]. Available: http://thearmsguide.com/wp-content/uploads/2013/11/Yaw-of-repose.jpg. [Accessed 3 September 2015].

[18] [Online]. Available: http://en.wikipedia.org/wiki/Field_artillery_team#/media/File:785px-Arty_Call_for_Fire_1.jpg. [Accessed 3 September 2015].